EXTENSION OF PROBABILISTIC GAIN, PHASE, DISK AND DELAY MARGINS FOR MULTI-INPUT MULTI-OUTPUT SPACE CONTROL SYSTEMS*

Franca Somers[(1)], Clément Roos[(2)], Francesco Sanfedino[(3)], Samir Bennani[(4)], Valentin Preda[(5)]

[(1)]*ONERA, The French Aerospace Lab, Toulouse, France, email: franca.somers@onera.fr*
[(2)]*ONERA, The French Aerospace Lab, Toulouse, France, email: clement.roos@onera.fr*
[(3)]*ISAE SUPAERO, Université de Toulouse, France, email: francesco.sanfedino@isae-supaero.fr*
[(4)]*ESA ESTEC, Noordwijk, The Netherlands, email: samir.bennani@esa.int*
[(5)]*ESA ESTEC, Noordwijk, The Netherlands, email: valentin.preda@esa.int*
*This work is part of the OSIP 4000134724 supported by ESA.

ABSTRACT

Current validation and verification (V&V) activities in the aerospace industry typically rely on time-consuming simulation-based tools. These tools can provide a probability measure for sufficiently frequent phenomena, but may fail to detect rare but critical combinations of parameters. As the complexity of modern space systems increases, this limitation plays an increasing role. In recent years, model-based worst-case analysis methods have reached maturity. Without requiring simulations, these tools can fully explore the space of all possible uncertain parameter combinations, and provide guaranteed mathematical bounds on robust stability margins and worst-case performance levels. However, they give no measure of probability and may therefore be overly conservative. Conversely, probabilistic μ-analysis combines worst-case information with probability measure. As such, it tends to bridge the analysis gap between Monte Carlo simulations and deterministic worst-case approaches. The latest developments in probabilistic μ-analysis have all been devoted to stability margins for Single-Input Single-Output (SISO) systems. This paper addresses the extension of probabilistic gain, phase, disk and delay margins to multi-variable analysis for Multi-Input Multi-Output (MIMO) control systems. To validate the proposed approach, an in-depth analysis is conducted on an academic benchmark. The analysis capability for higher-order systems is also evaluated on two more realistic satellite models.

1 INTRODUCTION

Stability margins can be seen as "safety factors" to account for the mismatch between the plant model used for control design and the dynamics of the real system [17]. The gain and phase margins are the most widely used in the industry. Originally dedicated to the study of SISO systems, they are also commonly applied to MIMO systems via a loop-at-a-time analysis [10]. However, such an approach can lead to wrong conclusions, as it fails to capture the effect of simultaneous perturbations occurring in multiple channels [17]. Over the years various solutions to account for this issue have been proposed. Several early researches present methods to study the stability of nominal MIMO systems perturbed by simultaneous gain and phase disturbances, as well as ways to determine the maximum acceptable simultaneous changes in both gain and phase of each channel [1]–[3], [8]. The first of these studies, [2], provides a very conservative measure of robustness using singular values of the return difference matrix. [1] and [3] then present the subsequent efforts to reduce this conservatism. But all these methods fail to exactly evaluate the stability margin for MIMO systems. In contrast,

[8] provides an analysis method for exact evaluation of the stability margins by means of the minus inverse vector, defined as the negative value of the inverse of the open-loop transfer function. A more recent solution is disk margin analysis, to which a clear theoretical introduction is given in [17]. This margin accounts for simultaneous gain and phase variations and is suitable for MIMO system analysis [17]. Furthermore, in contrast to the prior described techniques, the disk margin fits better in more general robustness frameworks, such as structured singular value and integral quadratic constraints analysis. This makes it more straightforward to move into the analysis of uncertain systems. Similarly, the traditional – non-simultaneously evaluated – gain and phase margins can be easily coupled with these robustness analysis tools. As an example, an efficient method for independent robust MIMO gain or phase margin analysis using μ-analysis tools can be found in [13]. But besides gain and phase perturbations, most realistic control engineering problems also suffer from time delays. Since these time delays can have serious consequences for system stability, a lot of research on delayed systems and time-delay margins in both time and frequency domains, and in the presence of nominal and uncertain plants, is readily available, see e.g. [7], [9], [12]. All of the above described tools are of deterministic origin. On the contrary, in [20] and [22] probabilistic evaluations of the gain, phase, disk and delay margins for SISO systems were presented. Each of these probabilistic stability margins is computed by means of μ-analysis techniques. They benefit from the fact that, unlike Monte Carlo, μ-analysis is simulation-free and by providing formal stability/performance certificates in the frequency domain, no rare scenarios are missed. On top of that, these probabilistic μ-analysis tools overcome the conservatism provided by their deterministic counterpart by capturing the small probability of rare but possibly critical configurations corresponding to the tails of the probability distributions of potential scenarios [5]. Nevertheless, most industrial problems involve MIMO systems, influenced by multiple simultaneous perturbations on each Input-Output (IO)-channel. The main goal of this work is to extend the probabilistic SISO gain, phase, disk and delay margin algorithms of [20] and [22] to MIMO multi-variable system analysis. The interest of adopting these tools is twofold: to reduce the conservatism of loop-at-a-time analysis and to provide a framework to analyze more realistic scenarios.

The paper is organized as follows. The considered problem is first stated in Section II. Section III gives a brief overview to the proposed solution. The main theoretical results are then detailed in Section IV, together with their practical implementation. To demonstrate the capabilities of the developed tools, the proposed algorithms are finally applied to the analysis of 3 spacecraft benchmarks in Section V.

2 PROBLEM STATEMENT

Let us consider the following continuous-time uncertain Linear Time Invariant (LTI) system:

$$\begin{cases} \dot{\mathbf{x}} &= A(\delta)\mathbf{x} + B(\delta)\mathbf{u} \\ \mathbf{y} &= C(\delta)\mathbf{x} + D(\delta)\mathbf{u} \end{cases} \tag{1}$$

The real uncertain parameters $\delta = (\delta_1, \ldots, \delta_N)$ are bounded and without loss of generality normalized, so that the whole set of admissible uncertainties is covered when $\delta \in \mathcal{B}_\delta = [-1\ 1]^N$. They are independent random variables, whose probability density functions f are supported on the bounded interval $[-1\ 1]$. It is assumed that $A(\delta)$, $B(\delta)$, $C(\delta)$, $D(\delta)$ are polynomial or rational functions of the δ_i and that system (1) can be transformed into a Linear Fractional Representation (LFR) as shown in Figure 1a: the uncertainties are separated from the nominal LTI system $M(s)$ and isolated in a block-diagonal operator $\Delta = \text{diag}(\delta_1 \mathbf{I}_{n_1}, \ldots, \delta_N \mathbf{I}_{n_N}) \in \mathbb{R}^{p \times p}$ where $\mathbf{I}_{n_i}$ is the $n_i \times n_i$ identity matrix. The set of matrices with the same block-diagonal structure as Δ is denoted $\mathbf{\Delta}$. Let $\mathcal{B}_{\mathbf{\Delta}} = \{\Delta \in \mathbf{\Delta} : \delta_i \in \mathcal{B}_\delta\}$ and $D_{\mathbf{\Delta}} = \{\Delta \in \mathbf{\Delta} : \delta_i \in D\}$ be the subsets of $\mathbf{\Delta}$ corresponding to $\mathcal{B}_\delta$ and to a given box $D \in \mathcal{B}_\delta$ respectively. Finally, $\mathbf{u} \in \mathbb{R}^K$ and $\mathbf{y} \in \mathbb{R}^K$ represent the system inputs and outputs.

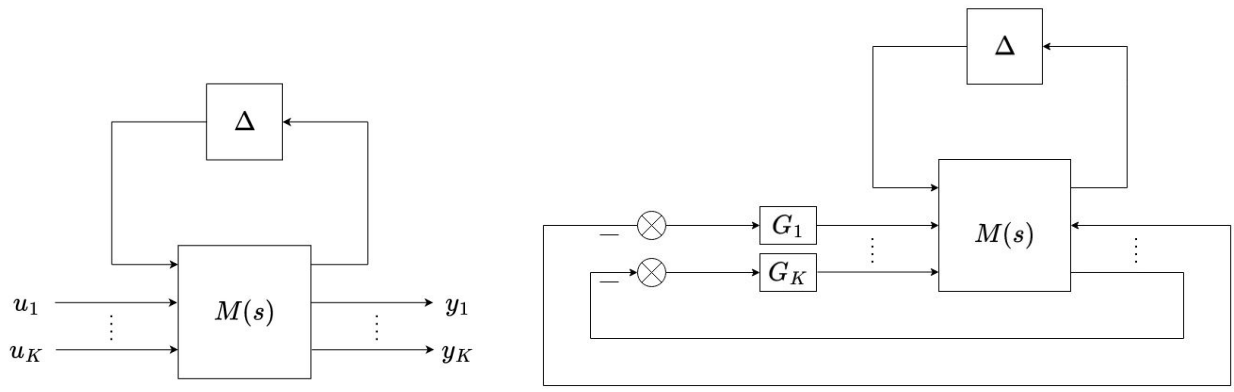

(a) Linear Fractional Representation (LFR) (b) Feedback loop for stability margin analysis

Figure 1: Standard system representations

In this work, system (1) and Figure 1a describe a control loop opened at the places where multiple stability margins should be simultaneously evaluated. The closed-loop interconnection is therefore recovered by applying a unit negative feedback between $\mathbf{y}$ and $\mathbf{u}$, *i.e.* by setting $G_k = 1$ for all $k \in [1 \dots K]$ in Figure 1b. A gain shift, a phase shift or a time-delay G_k, bounded by ϕ_k and whose expression is detailed in Section 4, is now introduced on each channel in accordance with the considered robustness specifications. Within this framework, **multi-variable probabilistic robust stability margins analysis** can be formalized as follows, where $\phi = [\phi_1 \ \dots \ \phi_K]^T$:

Problem 2.1 *Compute the probability $\overline{P}^{\phi}_{\mathbf{\Delta},f}(M(s))$ that there exists a combination of gain shifts, phase shifts and/or time-delays $G_1, \dots, G_K$ bounded by $\phi_1, \dots, \phi_K$ which makes the interconnection of Figure 1b unstable when Δ takes its values in $\mathcal{B}_{\mathbf{\Delta}}$ according to the probability density functions f.*

The considered control system can then be rejected or validated depending on whether $\overline{P}^{\phi}_{\mathbf{\Delta},f}(M(s))$ does or does not exceed a given threshold ϵ. A practical approach is presented in Section 4 to compute tight bounds on $\overline{P}^{\phi}_{\mathbf{\Delta},f}(M(s))$. The global underlying idea is first summarized in Section 3.

3 OVERVIEW OF THE PROPOSED SOLUTION

The STOchastic Worst-case Analysis Toolbox (STOWAT) is a toolbox dedicated to probabilistic μ-analysis, developed by ONERA. The original version of the toolbox, described in [16] and [18], only allowed for probabilistic robust stability and H_∞ performance analysis. However, for the STOWAT to be fully convincing for industry, it should be as efficient and versatile as possible. For this purpose, focus has since then been placed on improving the code [19]. Furthermore, the toolbox was recently equipped with four probabilistic stability margin algorithms, devoted to probabilistic gain, phase, disk and delay margin analysis for SISO systems [20], [22]. All four can be classified as μ-analysis based Branch-and-Bound (B&B) algorithms. μ-analysis requires as a preliminary step to transform the interconnection of Figure 1b into an LFR, which requires $G = G_1$ (note that there is only one single perturbation for SISO systems), to be a rational expression. The considered margin is first evaluated at the center of $\mathcal{B}_\delta$, *i.e.* for the nominal system $\Delta = 0$. If it is larger (resp. smaller) than the desired threshold $\phi = \phi_1$, it is then checked whether the stability margin requirement is satisfied (resp. violated) on the entire domain $\mathcal{B}_\delta$ using sufficient conditions involving μ upper bound computations. If this cannot be guaranteed, $\mathcal{B}_\delta$ is finally partitioned into smaller boxes and this process is repeated until each box has guaranteed sufficient/insufficient margin, or is small enough to be

neglected. Guaranteed upper and lower bounds on the exact probability of stability margin violation $\overline{P}^{\phi}_{\mathbf{\Delta},f}(M(s))$ are finally obtained, based on the probability distributions of the uncertain parameters δ. These stability margin tools are limited to SISO system analysis. But since most industrial problems involve MIMO systems, perturbed by various types of disturbances, the main contribution of this paper is the adaptation of the algorithms for MIMO system analysis. Furthermore, a complete design freedom is introduced by allowing multi-variable margin analysis, in other words, various types of margins can simultaneously be considered for each IO-channel.
The core of the existing stability margin algorithms remains the same. Only two main modifications are required: additional matrix operations are needed to construct the perturbed system used by the B&B algorithm, and new conditions are introduced to determine whether the satisfaction test or the violation test should be applied. For SISO systems, these conditions mostly rely on grid-based methods. However in [20], it was already shown that gridding is usually very efficient for SISO and loop-at-a-time margin analysis, but gets significantly slower if the number of IO-channels increases. An alternative and much more efficient approach for MIMO systems, using μ-based tools, was already proposed for disk margin analysis in [20]. In Section 4.3, it is justified why slight modifications of this approach are required here for multi-variable analysis. Furthermore, it is well-known that purely real μ-analysis problems are often more time-consuming and sometimes yield more conservative results than complex ones. Therefore, a total of two MIMO multi-variable margin analysis algorithms with different methods to determine whether the violation or satisfaction test should be used, are developed. One uses a grid-based search and the other uses a μ-based approach. Both algorithms are implemented in the STOWAT and their performance is evaluated in Section 5.

4 PROBABILISTIC MIMO MULTI-VARIABLE MARGINS

4.1 Interconnection for MIMO Multi-variable margin analysis

As already mentioned, the expression of G_k in Figure 1b depends on the margin considered for the IO-channel from u_k to y_k. Expressions corresponding to individual margins are introduced in [20] and [22], and are shortly recalled below for completeness. Note that, more generally, G_k can be constructed by multiplying the respective expressions for the involved individual margins, if multiple margins are evaluated in series.

- The gain margin $\mathcal{M}_g$ is the largest gain variation before the closed-loop system becomes unstable. G_k is therefore a real number which belongs to the interval:

$$G_k \in \left[10^{-\frac{\phi_k}{20}}\ 10^{\frac{\phi_k}{20}}\right] \subset \mathbb{R} \tag{2}$$

  where ϕ_k is the desired gain margin in dB. It is normalized as follows:

$$G_k = G_{d_k}\delta_{m_k} + G_{n_k}\ ,\ \begin{cases} G_{d_k} = 0.5\left(10^{\frac{\phi_k}{20}} - 10^{-\frac{\phi_k}{20}}\right) \\ G_{n_k} = 0.5\left(10^{\frac{\phi_k}{20}} + 10^{-\frac{\phi_k}{20}}\right) \end{cases} \tag{3}$$

  such that G_k exactly covers the interval (2) when $\delta_{m_k} \in \mathbb{R}$ covers the normalized interval $[-1\ 1]$.

- The phase margin $\mathcal{M}_p$ is the largest phase variation before the closed-loop system becomes unstable. G_k is therefore a complex number of modulus 1 defined as:

$$G_k = e^{j\tilde{\phi_k}}\ ,\ \tilde{\phi_k} \in \left[-\frac{\pi\phi_k}{180}\ \frac{\pi\phi_k}{180}\right] \subset \mathbb{R} \tag{4}$$

where ϕ_k is the desired phase margin in deg. When defined as in (4), G_k does not depend on ϕ_k in a rational way, which prevents the interconnection of Figure 1b from being represented as a LFR. The following alternative but equivalent rational formulation is therefore used instead:

$$G_k = \frac{1 + j\tilde{\delta}_k}{1 - j\tilde{\delta}_k} \quad , \quad \tilde{\delta}_k \in \left[-\tan\frac{\pi\phi_k}{360} \;\; \tan\frac{\pi\phi_k}{360} \right] \subset \mathbb{R} \tag{5}$$

The last step is to normalize $\tilde{\delta}_k$ as follows:

$$\tilde{\delta}_k = \tan\frac{\pi\phi_k}{360}\delta_{m_k} \tag{6}$$

so that G_k in equation (5) exactly covers the circle arc (4) in the complex plane when $\delta_{m_k} \in \mathbb{R}$ covers the normalized interval $[-1\ 1]$.

- The disk margins $\mathcal{M}_d^\sigma$ account for simultaneous gain and phase variations. Using the parameterization introduced in [17], $G_k(s)$ is a complex number defined as:

$$G_k = \frac{1 + \frac{1-\sigma_k}{2}\tilde{\delta}_k}{1 - \frac{1+\sigma_k}{2}\tilde{\delta}_k} \quad , \quad |\tilde{\delta}_k| \leq \phi_k \quad , \quad \tilde{\delta}_k \in \mathbb{C} \tag{7}$$

where $\phi_k < 2/|1 + \sigma_k|$ is the desired disk margin. This condition ensures that the set of all admissible $G_k(s)$ forms a disk $\mathcal{D}(\phi_k, \sigma_k) \subset \mathbb{C}$ centered on the real axis, with skew parameter $\sigma_k \in \mathbb{R}$. For a given value of σ_k, $\mathcal{M}_d^{\sigma_k}$ is the largest value of ϕ_k such that the closed-loop system is stable for all $G_k \in \mathcal{D}(\phi_k, \sigma_k)$. $\tilde{\delta}_k$ can then be normalized as follows:

$$\tilde{\delta}_k = \phi_k\, \delta_{m_k} \tag{8}$$

so that G_k exactly covers the disk $\mathcal{D}(\phi_k, \sigma_k)$ when $\delta_{m_k} \in \mathbb{C}$ covers the unit disk $d = \{z \in \mathbb{C} : |z| \leq 1\}$.

- The delay margin $\mathcal{M}_\tau$ is the largest delay that can be introduced before the closed-loop system becomes unstable. The delay margin can be interpreted as a frequency dependent phase shift, and is thus also represented by an exponential term, $G_k(s) = e^{-\tau_k s}$, $\tau_k \in [0\ \phi_k]$. For the sake of creating an LFR, the exponential term should be replaced by a rational expression. In [22], two replacements are introduced. For the delay margin *satisfaction test*, a function with the same properties (unit gain and phase varying linearly with frequency) as the actual time delay is used:

$$G_k = \frac{2j\delta_{m_k}^2 - 2(1+j)\delta_{m_k} + 1}{-2j\delta_{m_k}^2 - 2(1-j)\delta_{m_k} + 1} \tag{9}$$

for which:

$$\delta_{m_{k_{max}}}(\omega) = \begin{cases} \dfrac{1 - \beta_k - \sqrt{1+\beta_k{}^2}}{2} & \text{if} \quad \omega < \pi/\phi_k \\ 0.5 & \text{if} \quad \omega = \pi/\phi_k \\ \dfrac{1 - \beta_k + \sqrt{1+\beta_k{}^2}}{2} & \text{if} \quad \omega > \pi/\phi_k \end{cases} \tag{10}$$

and $\beta_k = \tan\frac{-\min(\phi_k\omega, 2\pi)}{2}$. Special attention is needed as $\delta_{m_k} \in [0, \delta_{m_{k_{max}}}(\omega)]$ has a frequency dependent upper bound. This makes direct use of standard μ-tools impossible. A solution was proposed in [22] and is recalled here in Section 4.2. The *violation test* calls for another approach. Indeed, it requires fixing δ_{m_k} values on the whole frequency range as explained in

Section 4.3, which is not possible with the above formlulation since the upper bound on δ_{m_k} is frequency dependent. Therefore a second order Padé approximation (11) is used as alternative replacement function:

$$G_k(s) = \frac{(\tau_k s)^2 - 6\tau_k s + 12}{(\tau_k s)^2 + 6\tau_k s + 12} \tag{11}$$

where for normalization reasons $\tau_k = \frac{\phi_k}{2}(\delta_{m_k} + 1)$ and $\delta_{m_k} \in [-1\ 1]$.

Standard matrix manipulations based on the Redheffer star product then allow to transform the interconnection of Figure 1b into that of Figure 2, where $\Delta_m = \text{diag}(\delta_{m_1} I_{m_1} \dots \delta_{m_K} I_{m_K}) \in \mathcal{B}_{\mathbf{\Delta_m}}$. Here δ_{m_k} is real (resp. complex) for gain/phase/delay (resp. disk) margins. It belongs to $[-1\ 1]$ for gain and phase margins, $d = \{z \in \mathbb{C} : |z| \leq 1\}$ for disk margin, and either $[0\ \delta_{m_{k_{max}}}(\omega)]$ or $[-1\ 1]$ for the delay margin depending on whether the satisfaction test or the violation test is applied. Finally, $m_k = 1$ (resp. 2) for gain/phase/disk (resp. delay) margins.

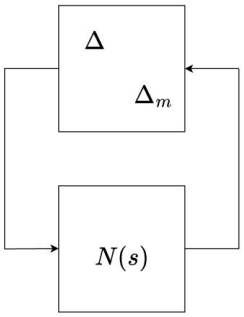

Figure 2: Transformation of the interconnection of Figure 1b

4.2 Checking stability margin satisfaction on a box

Let us consider a box $D \in \mathcal{B}_\delta$. The interconnection $N(s) - \text{diag}\,(\Delta, \Delta_m)$ of Figure 2, with $\Delta \in D_{\mathbf{\Delta}}$ and $\Delta_m \in \mathcal{B}_{\mathbf{\Delta_m}}$, is normalized and equivalently replaced by $\tilde{N}(s) - \text{diag}\,(\tilde{\Delta}, \Delta_m)$, with $\tilde{\Delta} \in \mathcal{B}_{\mathbf{\Delta}}$. Checking whether the stability margin requirements are satisfied on the entire box D can then be done using the necessary and sufficient condition of Proposition 4.1.

Proposition 4.1 *All stability margins are guaranteed to be larger than ϕ on a given box $D \subset \mathcal{B}_\delta$ if and only if the interconnection $\tilde{N}(s) - \text{diag}\,(\tilde{\Delta}, \Delta_m)$ is stable $\forall \tilde{\Delta} \in \mathcal{B}_{\mathbf{\Delta}}$ and $\forall \Delta_m \in \mathcal{B}_{\mathbf{\Delta_m}}$.*

If the analysis does not include delay margin requirements, all δ_{m_k} are normalized and Proposition 4.1 reduces to a standard μ-analysis problem (see *e.g.* [4], [6], [20]), which can be solved using existing tools such as the SMART Library of the SMAC Toolbox [14]. In this case, the condition of Proposition 4.1 is equivalent to:

$$\mu(\tilde{N}(j\omega)) < 1\ \forall \omega \in \mathbb{R}. \tag{12}$$

But if delay margin requirements are specified, Proposition 4.1 requires solving a non-standard μ-analysis problem due to the presence of some δ_{m_k} with frequency-dependent upper bounds. Using the Hamiltonian-based method of [11], [22] proposes a three-step strategy to compute a whole frequency interval $[\omega_{min}\ \omega_{max}]$ on which a μ upper bound computed at a given frequency ω_k remains valid, when a single uncertainty has frequency-dependent bounds (*i.e.* in case of a single delay margin requirement). A generalization is proposed in Algorithm 1 below in case of multiple delays.

Algorithm 1 Validity interval $[\omega_{min}\ \omega_{max}]$ around ω_k

Step 1 - Initialization:

1. select a frequency ω_k for which stability has not been evaluated yet and normalize the frequency dependent δ_{m_k} with respect to the corresponding desired ϕ_k at ω_k to get the fully normalized interconnection $\tilde{N}(s) - \text{diag}\,(\tilde{\Delta}, \Delta_m)$, $\tilde{\Delta} \in \mathcal{B}_{\mathbf{\Delta}}$, and $\Delta_m \in \mathcal{B}_{\mathbf{\Delta_m}}$.
2. check whether $\overline{\mu}(\tilde{N}(j\omega_k)) \leq 1$
3. **if** not **then** STOP **else** compute an initial interval $[\omega_{min}\ \omega_{max}]$ around ω_k on which $\overline{\mu}(\tilde{N}(j\omega)) \leq 1$

Step 2 - Lower bound improvement:

initialization: set $\omega_{test} = \omega_k$
while $\omega_{test} - \omega_{min} > \epsilon$ **do**

1. set $\omega_{test} = \omega_{min}$
2. normalize each frequency dependent δ_{m_k} at ω_{test} and compute $\tilde{N}(s)$
3. compute an interval $[\omega_1\ \omega_2]$ around ω_{test} on which $\overline{\mu}(\tilde{N}(j\omega)) \leq 1$
4. set $\omega_{min} = \omega_1$

end while

Step 3 - Upper bound improvement:

initialization: set $\omega_{low} = \omega_k$ and $\omega_{high} = \omega_{max}$
while $\omega_{high} - \omega_{low} > \epsilon$ **do**

1. set $\omega_{test} = \frac{(\omega_{high}+\omega_{low})}{2}$
2. normalize each frequency dependent δ_{m_k} at ω_{test} and compute $\tilde{N}(s)$
3. check whether the D and G scaling matrices associated to the μ upper bound computed at step 1 are still valid at ω_{low}
4. **if** valid **then**
   - determine the validity interval $[\omega_1\ \omega_2]$ using the Hamiltonian-based algorithm of [11]
   - **if** $\omega_2 > \omega_{test}$ **then** set $\omega_{max} = \omega_{test}$ and $\omega_{low} = \omega_{test}$ **else** set $\omega_{high} = \omega_{test}$

end while

4.3 Checking stability margin violation on a box

As the second order Padé approximation (11) is used instead of the exact replacement function (9) for time-delay perturbed systems, no uncertainties with frequency dependent upper bounds appear in Δ_m, which only contains normalized δ_{m_k} belonging to $[-1, 1]$ or d depending on the considered margins. Therefore, in contrast to the satisfaction test, no special approach is needed for the violation test if time delays need to be taken into account. Checking whether any of the stability margin requirements is violated on an entire box $D \subset \mathcal{B}_\delta$ can be done using Proposition 4.2.

Proposition 4.2 *Any of the stability margins is guaranteed to be lower than ϕ on a given box $D \subset \mathcal{B}_\delta$ if $\forall \tilde{\Delta} \in \mathcal{B}_{\mathbf{\Delta}}$, $\exists\, \hat{\Delta}_m = diag(\delta_{m_1} I_{m_1} \ldots \delta_{m_K} I_{m_K}) \in \mathcal{B}_{\mathbf{\Delta_m}}$ such that the interconnection $\tilde{N}(s) - diag\,(\tilde{\Delta}, \hat{\Delta}_m)$ is unstable.*

The condition in Proposition 4.2 is only sufficient in the general case, but becomes also necessary when no delay margin requirements are considered. Indeed, the characterizations (2), (5) and (7)

used for the gain, phase and disk margins are exact, unlike the Padé approximation (11) used for the delay margin, which is only an approximation. In all cases, the condition in Proposition 4.2 cannot be directly evaluated using μ-based tools. It is thus replaced with the sufficient condition of Proposition 4.3, which basically consists of choosing the same value of $\hat{\Delta}_m$ for all $\tilde{\Delta} \in \mathcal{B}_{\mathbf{\Delta}}$.

Proposition 4.3 *Any of the stability margins is guaranteed to be lower than ϕ on a given box $D \subset \mathcal{B}_\delta$ if $\exists\, \hat{\Delta}_m \in \mathcal{B}_{\mathbf{\Delta_m}}$ such that the interconnection $\tilde{N}(s) - diag\,(\tilde{\Delta}, \hat{\Delta}_m)$ is unstable $\forall \tilde{\Delta} \in \mathcal{B}_{\mathbf{\Delta}}$.*

Once $\hat{\Delta}_m$ is determined, it remains constant in Proposition 4.3 and can therefore be integrated into $\tilde{N}(s)$ to form a reduced normalized interconnection $\tilde{N}_r(s) - \tilde{\Delta}$. Verifying the sufficient condition of Proposition 4.3 then consists of evaluating the instability of $\tilde{N}_r(s) - \tilde{\Delta}$ on $\mathcal{B}_{\mathbf{\Delta}}$, which can be done using existing μ-based tools such as the SMART Library. The search for $\hat{\Delta}_m$ (if it exists at all) is the most critical aspect of the algorithm. All admissible values of Δ_m that make the reduced nominal system $\tilde{N}_r(s)$ unstable are potential candidates. A logical strategy is therefore to study the stability of the interconnection $\tilde{N}(s) - \text{diag}\,(0_{p\times p}, \Delta_m)$. Two solutions are proposed in the present work: a μ-based and a grid-based approach.

The idea behind the μ-based approach is similar to the one presented for disk margin analysis in [20]: search for the value of $\Delta_m \in \mathcal{B}_{\mathbf{\Delta_m}}$, which moves a pole of $\tilde{N}(s) - \text{diag}\,(0_{p\times p}, \Delta_m)$ as far as possible in the right half-plane. This can be done by gradually shifting the stability axis into the right half-plane and computing the smallest destabilizing perturbation Δ_m using μ-based algorithms. It should however be noted that the choice of the most suitable algorithm depends on the structure of Δ_m. Indeed, systems with pure real, pure complex or mixed uncertainties require different algorithms (pole migration techniques in the first case, power algorithms in the others), for applicability, efficiency and accuracy reasons [15]. Here a distinction is thus made between MIMO disk margin analysis (complex uncertainties only), MIMO gain, phase and/or delay margin analysis (real uncertainties only) and the general case (mixed real/complex uncertainties). The iterative process is stopped as soon as one of the δ_{m_k} reaches a magnitude of 1. Note that if no disk margin requirements need to be evaluated, no complex uncertainties are considered. Therefore, the determination of $\hat{\Delta}_m$ might sometimes be time consuming and overly conservative, but this remains rare in practice.

For the grid-based approach, a finite number of values are considered for each δ_{m_k}. For real uncertainties, the grid covers the interval $[-1\ 1]$, and for complex uncertainties, values on the unit disk are considered. In the end, the value of Δ_m is selected, which moves one pole of $\tilde{N}(s) - \text{diag}\,(0_{p\times p}, \Delta_m)$ as far as possible in the right half-plane. The risk with such an approach is to fail to identify an unstable configuration, although there exists one between some points of the grid. However, this has no other consequence than unnecessarily splitting the box D when applying the branch-and-bound (B&B) algorithm of Section 4.4, which might slightly increase the computational time. More problematic is that the computational time is an exponential function of the number of margin requirements, *i.e.* the number of δ_{m_k} in Δ_m. For low numbers (typically < 3) of margin requirements, the grid-based method is however more efficient than the μ-based approach.

4.4 Algorithmic issues

The conditions for determining whether a given MIMO multi-variable stability margin requirement is satisfied (Proposition 4.1) or violated (Proposition 4.3) on an entire box are now integrated into a B&B scheme described in Algorithm 2, and inspired by the ones presented in [16], [20]. The domain of guaranteed stability $D_s \subset \mathcal{B}_\delta$ is partitioned as follows:

$$D_s = D_m \cup D_{\overline{m}} \cup D_{m_u} \tag{13}$$

where D_m, $D_{\overline{m}}$ and D_{m_u} are the domains of guaranteed margin satisfaction, guaranteed margin violation and undetermined margin respectively, with probabilities $p(D_m)$, $p(D_{\overline{m}})$ and $p(D_{m_u})$. The

investigated domain is limited to D_s, since stability margins analysis only makes sense for stable systems. A preliminary stability analysis is therefore performed with Algorithm 1 of [16], leading to:

$$\mathcal{B}_\delta = D_s \cup D_{\overline{s}} \cup D_{s_u} \tag{14}$$

where $D_{\overline{s}}$ and D_{s_u} are the domains of guaranteed instability and undetermined stability respectively. The following partition of $\mathcal{B}_\delta$ is finally obtained by combining (13)-(14):

$$\mathcal{B}_\delta = D_m \cup D_{\overline{m}} \cup D_{m_u} \cup D_{\overline{s}} \cup D_{s_u} \tag{15}$$

This leads to guaranteed bounds on the exact probability $\overline{P}^{\phi}_{\mathbf{\Delta},f}(M(s))$ of stability margin violation, thus solving Problem 2.1:

$$p(D_{\overline{m}}) \leq \overline{P}^{\phi}_{\mathbf{\Delta},f}(M(s)) \leq p(D_{\overline{m}}) + p(D_{m_u}) = p(D_s) - p(D_m)$$

where the probabilities are computed with the method proposed in [16].

5 NUMERICAL RESULTS

In this section three benchmarks are used to numerically validate the proposed algorithms. Section 5.1 first demonstrates the capabilities and limitations of the code through the analysis of a simple satellite model with two uncertainties, adapted from [4]. The low number of uncertainties allows for graphical representations of the results, which underpin the conclusions and enhance clarity. Afterwards, in Section 5.2, the applicability of the tool to more advanced models with more states and uncertainties is put to the test. All computational times reported in this paper were obtained using Matlab R2022b running serially on a single core on a Windows 10 laptop from 2021 with an Intel Core i7-1165G7 CPU running at 3 GHz and 16 GB of RAM.

5.1 Academic spinning satellite benchmark

A symmetric cylinder spinning around its symmetry axis z with a constant rate Ω can be seen as a very simplified representation of a satellite. The angular rates ω_x and ω_y around the x and y axes are controlled using torques T_x and T_y. Let I_x, $I_y = I_x$ and I_z be the inertia of the satellite with respect to the x, y and z axes respectively. The system rotational motion can be described by:

$$\begin{cases} T_x = I_x\dot{\omega}_x - \omega_y\Omega(I_x - I_z) \\ T_y = I_x\dot{\omega}_y - \omega_x\Omega(I_z - I_x) \end{cases} \tag{16}$$

The systems dynamics can equally be described by the following state space representation $P(s)$:

$$\begin{bmatrix} \dot{\omega}_x \\ \dot{\omega}_y \end{bmatrix} = \begin{bmatrix} 0 & a \\ -a & 0 \end{bmatrix} \begin{bmatrix} \omega_x \\ \omega_y \end{bmatrix} + \begin{bmatrix} \delta_1 & 0 \\ 0 & \delta_2 \end{bmatrix} \begin{bmatrix} u_x \\ u_y \end{bmatrix} \tag{17}$$

where $a = \omega\left(1 - \frac{I_z}{I_x}\right)$,$u_x = \frac{T_x}{I_x}$ and $u_y = \frac{T_y}{I_x}$. Two uniformly distributed uncertain parameters $\delta_1 \in [-0.5, 2.5]$ and $\delta_2 \in [0, 2]$ have been introduced to represent possible variations of the control torques. Two measures ν_x and ν_y are available:

$$\begin{bmatrix} \nu_x \\ \nu_y \end{bmatrix} = \begin{bmatrix} 1 & a \\ -a & 1 \end{bmatrix} \begin{bmatrix} \omega_x \\ \omega_y \end{bmatrix} \tag{18}$$

Algorithm 2 Probabilistic multi-variable stability margin

$\mathcal{L} \leftarrow \{\mathcal{B}_\delta\}$ ▷ *list of all boxes left to investigate*
$D_m, D_{\overline{m}}, D_{m_u} \leftarrow \emptyset$
$p(D_m), p(D_{\overline{m}}), p(D_{m_u}) \leftarrow 0$
while $\mathcal{L} \neq \emptyset$ **do**
  extract the box $D \in \mathcal{L}$ with the highest probability
  compute the interconnection $\tilde{N}(s) - \text{diag}\,(\tilde{\Delta}, \Delta_m)$
  check if $\hat{\Delta}_m$ exists which makes $\tilde{N}_r(s)$ unstable
  if not **then** ▷ *nominal margin on D is $\geq \phi$*
    check margin satisfaction on D with Proposition 4.1
    if guaranteed **then**
      add D to D_m and set $p(D_m) \leftarrow p(D_m) + p(D)$
    else
      declare current iteration as inconclusive
    end if
  else ▷ *nominal margin on D is $< \phi$*
    check margin violation on D with Proposition 4.3
    if guaranteed **then**
      add D to $D_{\overline{m}}$ and set $p(D_{\overline{m}}) \leftarrow p(D_{\overline{m}}) + p(D)$
    else
      declare current iteration as inconclusive
    end if
  end if
  if current iteration is inconclusive **then**
    if $p(D) > p_{min}$ **then**
      select a direction for cutting D
      partition D and add the resulting boxes into $\mathcal{L}$
    else
      add D to D_{m_u} and set $p(D_{m_u}) \leftarrow p(D_{m_u}) + p(D)$
    end if
  end if
end while

and a static controller K is applied:

$$\begin{bmatrix} u_x \\ u_y \end{bmatrix} = -K \begin{bmatrix} \nu_x \\ \nu_y \end{bmatrix} = - \begin{bmatrix} 1 & -0.5 \\ 0 & 1 \end{bmatrix} \begin{bmatrix} \nu_x \\ \nu_y \end{bmatrix} \tag{19}$$

It is assumed in the sequel that $a = 5$. Since stability margins can only be determined for stable interconnections, a stability analysis is first performed on the uncertain closed-loop system (17)-(19) using Algorithm 1 of [16]. Afterwards a probabilistic MIMO phase margin analysis is performed using Algorithm 2. The closed-loop system is first opened at the plant inputs and transformed into the LFR of Figure 1a, where u_1/u_2 correspond to u_x/u_y in (17) and y_1/y_2 to u_x/u_y in (19). Two independent phase shifts G_1/G_2 are then added, whose maximum values are set to $\phi_1 = \phi_2 = \phi = 15°$. The B&B algorithm stops when $p(D) \leq p_{min} = 1/100\%$ for all $D \in \mathcal{L}$. With these settings, it can be determined with both the μ-based and grid-based versions of Algorithm 2 that:

1. 57.9% of the uncertainty domain $[-0.5\ 2.5] \times [0\ 2]$ is guaranteed to be stable in closed loop,

2. the probability of MIMO phase margin violation satisfies $\overline{P}^{\phi}_{\mathbf{\Delta},f}(M(s)) \in [9.8\%\ 12.2\%]$.

Figure 3 provides a graphical representation of the obtained results, with the following color code:

- green: stability is guaranteed for all phase shifts $\leq \phi \Rightarrow$ the MIMO phase margin is guaranteed to be $\geq \phi$,
- red: nominal stability (*i.e.* without phase shifts) is guaranteed, but there exist some phase shifts $\leq \phi$ which make the closed-loop system unstable $\Rightarrow$ the MIMO phase margin is guaranteed to be $< \phi$,
- blue: nominal stability is guaranteed, but it cannot be determined whether the MIMO phase margin is lower or higher than the desired threshold ϕ,
- orange: nominal instability is guaranteed,
- gray: nominal stability is undetermined.

The results are validated by means of a comparison with a classical grid-based approach:

- magenta: the MIMO phase margin is guaranteed to be $\geq \phi$,
- yellow: the MIMO phase margin is guaranteed to be $< \phi$,
- black: the system is unstable.

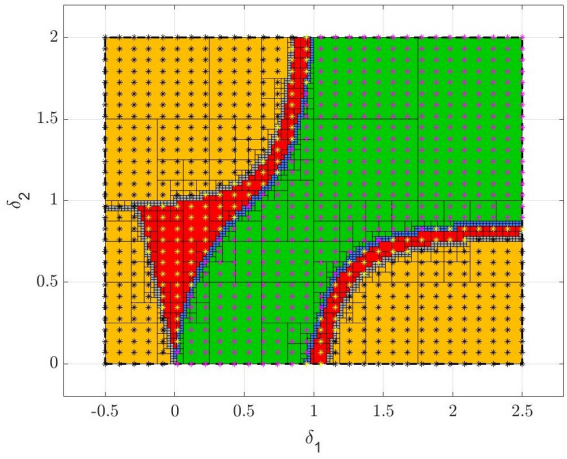

Figure 3: MIMO phase margin analysis

For this particular example, the grid-based and the μ-based tests used to compute $\hat{\Delta}_m$ in Algorithm 2 give results with similar accuracy, where accuracy refers to the size of the uncertainty domain for which the MIMO stability margin is undetermined (blue). However, there are examples where the grid-based method outperforms the μ-based one in terms of accuracy. The computed bounds on μ may indeed, as mentioned in Section 4.3, be too conservative when only real uncertainties are involved in Δ_m. Moreover, as the size of Δ_m is small, the grid-based approach is significantly faster compared to the μ-based one, $\sim$ 19 seconds vs $\sim$ 263 seconds. But the latter becomes much more efficient when the number of elements in Δ_m increases , since the computational time increases polynomial, instead of exponentially for the grid-based approach.
For the sake of comparison, and to emphasize the need for MIMO analysis tools, two loop-at-a-time analyses have been done as well. This means that each of the two channels of the control loop is

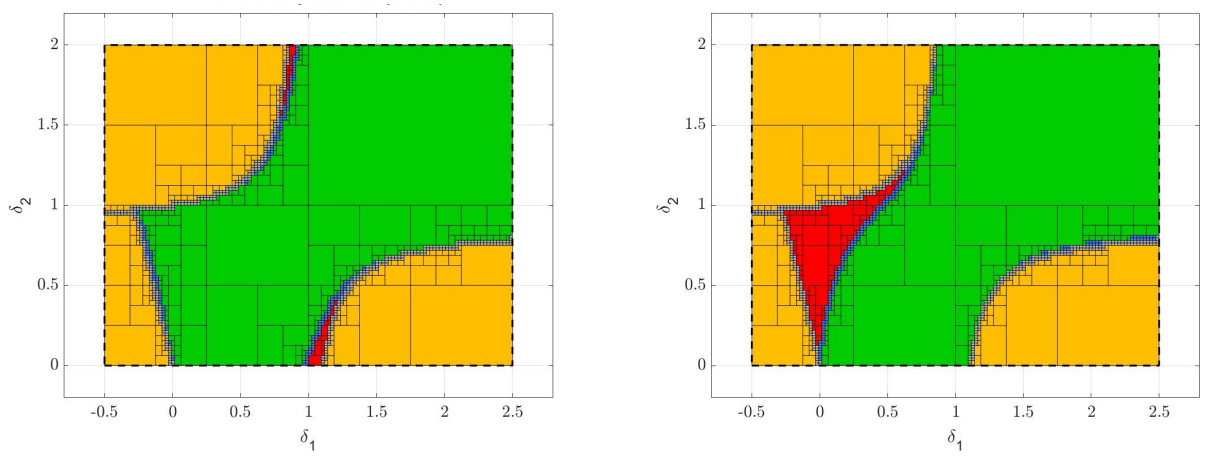

(a) x channel

(b) y channel

Figure 4: Loop-at-a-time phase margin analysis

successively opened, the other remaining closed. As such two SISO LFR are obtained for which a probabilistic phase margin analysis is performed using the grid-based version of Algorithm 2. It can be shown in less than 4 seconds that:

1. 57.9% of the uncertainty domain $[-0.5\ 2.5] \times [0\ 2]$ is guaranteed to be stable in closed loop,
2. the probability of phase margin violation satisfies $\overline{P}^{\phi}_{\mathbf{\Delta},f}(M(s)) \in [0.6\%\ \ 1.8\%]$ and $\overline{P}^{\phi}_{\mathbf{\Delta},f}(M(s)) \in [4.5\%\ 5.7\%]$ for the x and y channels respectively.

The comparison of Figures 4 and 5 shows that a significantly larger area is classified as margin violated if a true MIMO analysis is performed. In contrast to the loop-at-a-time analyses, the MIMO analysis accounts for the interaction between the different transfer channels. This method thereby prevents drawing wrong/overly optimistic conclusions.

5.2 More advanced satellite models

To demonstrate the applicability of the method to more complex systems, Algorithm 2 was also used to analyze two more realistic satellite models with flexible solar panels. The first model (Section 5.2.1) is a SISO model acquired from [20]. The second one (Section 5.2.2) is taken from [21] and concerns a MIMO system. The reader is referred to the original two papers for a detailed description of these models. In this section, just a brief description is provided, as the main focus is on probabilistic stability margin analysis.

5.2.1 SISO flexible satellite model [20]

The system considered in [20] is presented in Figure 5. It represents a satellite composed of a main body, two solar arrays (SA), an isolated payload (PL), and a reaction wheel (W) whose mass and inertia are neglected. The system is represented by a SISO model with 17 states containing in total 5 uniformly distributed parametric uncertainties related to the applied controller, the main body and the solar arrays, which significantly impact the flexible modes characteristics. The resulting LFR has a 10×10 Δ matrix.
In [20] the main control goal was to maintain a very high pointing accuracy despite flexible modes perturbations, *i.e.* minimize the influence of the perturbation Γ_{SA} on the pointing angle θ. Besides that, low control activity, disturbance rejection and good gain, phase and disk margins were also

required. Using Algorithm 1 of [20], it was established in a few seconds that $\mathcal{P}(\mathcal{M}_g < 3.2\,\text{dB}) < 10^{-4}$ for the gain margin, $\mathcal{P}(\mathcal{M}_p < 16\,deg) < 10^{-4}$ for the phase margin and $\mathcal{P}(\mathcal{M}_d^{\sigma=0} < 0.22) < 10^{-4}$ for the balanced disk margin, which seemed to demonstrate the reasonably good robustness properties of the system. It was also mentioned that the maximum gain and phase margins guaranteed by the disk margin, $M_g^d = 1.92\,\text{dB}$ and $M_p^d = 13\,deg$, are lower than those guaranteed by the separate gain and phase analyses, since stability is investigated for simultaneous gain and phase variations in the case of the disk margin. However, M_g^d and M_p^d are not simultaneously guaranteed, since the maximal gain shift is only guaranteed if the phase shift equals 0 and vice versa. These conclusions can be mitigated using the new probabilistic multi-variable stability margin analysis algorithm. Indeed, it can be proven in ~ 170 seconds using the grid-based version of Algorithm 2 that the probability that there exists at least one combination of gain / phase shifts lower than $1.92\,\text{dB}$ / $3\,^\circ$ which makes the system unstable is larger than 2%. This is not a rare event, which shows that the previous analysis was overly optimistic. Note that the computation time is relatively long, due to the large number of uncertainties, combined with a significant percentage of margin violation to be detected.

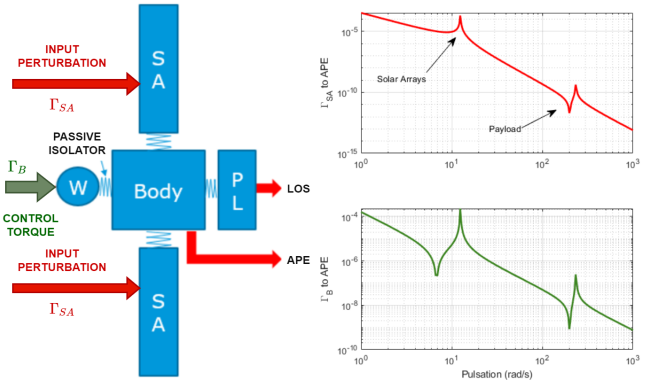

Figure 5: Simplified view of the nominal plant [20]

5.2.2 MIMO flexible satellite model [21]

Figure 6 presents the geometry of the system considered in [21]. It is a spacecraft consisting of a main body and two flexible solar panels. Here we study the controlled 3×3 transfer model between the external torques applied to the center of mass of the main body and its angular accelerations. The controller was designed to meet an Absolute Performance Error requirement in spite of low frequency orbital disturbances. And on top of that, to guarantee on each of the three system axes a gain margin $\mathcal{M}_g > 3$ (9.542 dB), a phase margin $\mathcal{M}_p > 38.9°$ and a disk margin $\mathcal{M}_d^{\sigma=1} > 0.667$. The model is of order 39, and contains in total 8 uniformly distributed uncertainties, leading to a very large Δ matrix of size 50×50, the solar arrays' rotation angle being repeated 32 times.
In [21] it was proven that the system violates the disk margin requirement for certain worst-case configurations. This conclusion was supported by both a deterministic and a probabilistic H_∞ performance analysis, requiring $\gamma < 1.5$. This specific γ namely simultaneously imposes the required gain, phase and disk margin. As the probabilistic H_∞ performance analysis tool is only suitable for SISO systems, three consecutive SISO analysis were done for the first, second and third IO-channel. The analysis on a very reduced frequency interval, centered around the worst-case frequency $[11, 12]$, indicated that the probability of margin violation was less then 0.5% for each of the three channels. The new MIMO multi-variable margin algorithm allows the MIMO gain, phase and disk margin to be studied one-by-one. It has the potential to provide more realistic results because the system interactions are taken into account. However, the current implementation is not yet efficient enough to provide sufficiently accurate results for this advanced model in a reasonable amount of time. As an example, after a probabilistic MIMO disk margin analysis of 3 hours, it can only be concluded that

$0 \leq \mathcal{P}(\mathcal{M}_d^{\sigma=1} > 0.667) \leq 0.38$. So there remains a big gap between the probability upper and lower bounds. Here the μ-based version of Algorithm 2 is used, which is for a system of this size already more efficient than the grid-based version. To reduce computational complexity, the satellite is studied with its solar panels fixed in the worst-case configuration, namely at an angle of -15°. This reduces the size of Δ to 18×18. However, further simplifications of the system are required to perform a more accurate analysis with the current code within an acceptable computational time. For example, model reduction could be applied or some system uncertainties could be fixed based on a sensitivity analysis. These are standard procedures also applied for time-consuming deterministic μ-analyses. Research is ongoing to improve efficiency when analyzing systems of this size and complexity.

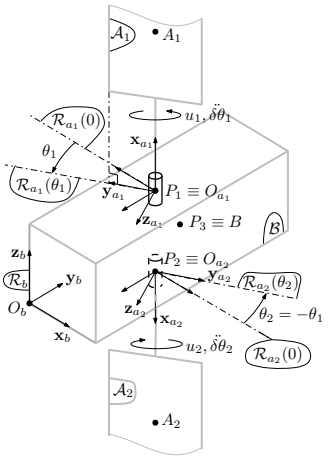

Figure 6: Spacecraft geometry

6 CONCLUSION

This paper presents the extension of the SISO gain, phase, disk and delay margin algorithms of [20] and [22] to a multi-variable stability margin algorithm for MIMO systems, which has been integrated into the STOchastic Worst-case Analysis Toolbox. The added value is highlighted by application to a simple academic benchmark, as well as two more complex satellite models. The new probabilistic μ-analysis algorithm indeed offers the possibility to analyze MIMO control systems as truthfully as possible. It both overcomes the possible conservatism of a deterministic worst-case approach, and avoids the need for time-consuming Monte-Carlo simulations by directly providing probabilistic stability measures. Ongoing research focuses on further improving the efficiency of the code.

REFERENCES

[1] U.-L. Ly, "Robustness analysis of a multi-loop flight control system," in *Proceedings of the AIAA, Guidance and Control Conference*, 1983.

[2] Y. Mukhopadhyay and J. Newsom, "A multiloop system stability margin study using matrix singular values," in *Proceedings of the AIAA, Guidance and Control Conference*, 1984.

[3] H.-H. Yeh, C. Ridgely, and S. Banda, "Nonconservative evaluation of uniform stability margins of multivariable feedback systems," in *Proceedings of the AIAA, 17th Fluid Dynamics, Plasma Dynamics, and Lasers Conference*, 1984.

[4] K. Zhou, J. Doyle, and K. Glover, *Robust and optimal control*. Prentice-Hall, New Jersey, 1996.

[5] S. Khatri and P. Parrilo, "Guaranteed bounds for probabilistic μ," in *Proceedings of the IEEE CDC*, 1998, pp. 3349–3354.

[6] G. Ferreres, *A practical approach to robustness analysis with aeronautical applications*. Springer, 1999.

[7] M. Jun and M. Safonov, "IQC robustness analysis for time-delay systems," *International Journal of Robust and Nonlinear Control*, vol. 11, no. 15, pp. 1455–1468, 2001.

[8] R. Katayanagi, "Exact evaluation of stability margin of multiloop flight control systems," *Journal of Guidance, Control, and Dynamics*, vol. 24, no. 1, pp. 137–140, 2001.

[9] K. Gu, V. Kharitonov, and J. Chen, *Stability of time-delay systems*. Springer Science, 2003.

[10] K. Åström and R. Murray, *Feedback systems - An introduction for scientists and engineers*. Princeton University Press, 2009.

[11] C. Roos and J.-M. Biannic, "Efficient computation of a guaranteed stability domain for a high-order parameter dependent plant," in *Proceedings of the American Control Conference*, 2010, pp. 3895–3900.

[12] F. Lescher and C. Roos, "Robust stability of time-delay systems with structured uncertainties a μ-analysis based algorithm," in *Proceedings of the IEEE Conference on Decision and Control*, 2011, pp. 4955–4960.

[13] C. Roos, F. Lescher, J.-M. Biannic, C. Doll, and G. Ferreres, "A set of μ-analysis based tools to evaluate the robustness properties of high-dimensional uncertain systems," in *Proceedings of the IEEE International Symposium on Computer-Aided Control System Design*, 2011.

[14] C. Roos, "Systems Modeling, Analysis and Control (SMAC) toolbox: An insight into the robustness analysis library," in *Proceedings of the IEEE Conference on Computer Aided Control System Design Conference*, available with the SMAC Toolbox at w3.onera.fr/smac/smart, 2013, pp. 176–181.

[15] C. Roos and J.-M. Biannic, "A detailed comparative analysis of all practical algorithms to compute lower bounds on the structured singular value," *Control Engineering Practice*, vol. 44, pp. 219–230, 2015.

[16] S. Thai, C. Roos, and J.-M. Biannic, "Probabilistic μ-analysis for stability and $\mathcal{H}_\infty$ performance verification," in *Proceedings of the American Control Conference*, 2019, pp. 3099–3104.

[17] P. Seiler, A. Packard, and P. Gahinet, "An introduction to disk margins [lecture notes]," *IEEE Control Systems Magazine*, vol. 40, no. 5, pp. 78–95, 2020.

[18] J.-M. Biannic, C. Roos, S. Bennani, F. Boquet, V. Preda, and B. Girouart, "Advanced probabilistic μ-analysis techniques for AOCS validation," *European Journal of Control*, vol. 62, pp. 120–129, 2021.

[19] C. Roos, J.-M. Biannic, and H. Evain, "A new step towards the integration of probabilistic μ in the aerospace V&V process," in *Proceedings of the 6th CEAS Conference on Guidance, Navigation and Control*, 2022.

[20] F. Somers, S. Thai, C.Roos, *et al.*, "Probabilistic gain, phase and disk margins with application to AOCS validation," in *Proceedings of the IFAC Symposium on Robust Control Design*, 2022.

[21] F. Sanfedino, D. Alazard, E. Kassarian, and F. Somers, "Satellite dynamics toolbox library: A tool to model multi-body space systems for robust control synthesis and analysis," in *Proceedings of the IFAC World Congress*, 2023.

[22] F. Somers, C. Roos, F. Sanfedino, S. Bennani, and V. Preda, "A μ-analysis based approach to probabilistic delay margin analysis of uncertain linear systems," in *Proceedings of the IEEE Conference on Control Technology and Applications*, 2023.